ISSN 1075-7015, Geology of Ore Deposits, 2006, Vol. 48, No. 5, pp. 384–401. © Pleiades Publishing, Inc., 2006.
Original Russian Text © A.A. Potseluev, D.I. Babkin, V.I. Kotegov, 2006, published in Geologiya Rudnykh Mestorozhdenii, 2006, Vol. 48, No. 5, pp. 439–459.

The Kalguty Complex Deposit, the Gorny Altai: Mineralogical and Geochemical Characteristics and Fluid Regime of Ore Formation

A. A. Potseluev, D. I. Babkin, and V. I. Kotegov

Tomsk Polytechnical University, pr. Lenina 30, Tomsk, 634050 Russia

Received November 9, 2005

Abstract—The results of detailed mineralogical, geochemical, and thermobarogeochemical studies of the Kalguty complex greisen deposit are presented. The chemical compositions of ore veins, greisens, and other geological bodies have been determined. A wide range of chemical elements from Li to U (48 elements, including noble metals and REE) has been determined in ore minerals. Graphite in association with quartz and sulfides was identified in ore veins for the first time. Graphite is enriched in a light carbon isotope. The $\delta^{13}C$ value varies from –26.3 ± 0.4 to –26.6 ± 0.3‰. High Au, Ag, Hg, Te, Sb, Bi, Cu, Pb, Zn, Fe, and S contents were detected in graphite grains with a microprobe. The graphite content increases regularly with depth; the spatial correlation of graphite with W, Mo, Cu, Au, Pt, Pd, and other metals is established. The highest Au, Ag, Pt, Pd, and Os contents are characteristic of minor intrusions of albitized granite porphyry ($\gamma\pi_2J_1vk$), intramineral dikes of hydrothermally altered kalgutite ($\gamma\pi_3J_1vk$), ore veins, their greisen selvages, and autonomous ore-bearing greisen bodies of the Mo stock type. Gold occurs in native form, while silver is contained largely in sulfides and sulfosalts. High PGE contents are characteristic of pyrite, wolframite, and molybdenite. The major components of fluid inclusions in quartz (H_2O, CO_2, CO, and H_2) have been studied, as well as hydrocarbons (CH_4, C_2H_6, C_3H_8, C_4H_{10}, C_5H_{12}, C_6H_{14}, C_2H_2, and C_2H_4) contained therein. Two-phase fluid inclusions are predominant, while single- and three-phase inclusions are less abundant. The homogenization temperatures of primary and secondary inclusions are 290–340 and 140–160°C, respectively. The concentration of dissolved salts (NaCl and KCl) in two-phase inclusions amounts to 11.6–14.0%. The H_2O and CO_2 contents decrease with depth, whereas the CO, H_2, and HC concentrations increase in the same direction. Graphite is regarded as a product of reactions with participation of fluid (gas) components. The ore mineralization was formed under contrasting conditions related to the oxidation of a primary reduced deep metalliferous fluid.

DOI: 10.1134/S1075701506050047

INTRODUCTION

Molybdenum–rare-metal–tungsten ore mineralization is widespread in the Gorny Altai, and the Kalguty deposit is a typical example (Fig. 1). The deposit has been studied since the 1930s and at present is the only thoroughly explored and mined deposit of this type in the region. The deposit is complex. In addition to tungsten and molybdenum as the major economic components, the Cu, Bi, and Be reserves have been estimated. The elevated noble metal concentrations in ore are notable. Special investigations allowed us to obtain new mineralogical and geochemical information and to consider the composition, genesis, and outlook of this deposit, unique in many respects, from a new viewpoint.

GEOLOGY

The Kalguty deposit is related both spatially and genetically to the pluton of Late Hercynian leucocratic rare-metal granites that bears the same name (Figs. 1, 2). The ore mineralization is represented by a series of steeply dipping wolframite–molybdenite–quartz veins with chalcopyrite, bismuthinite, and beryl. The length of veins varies from a few tens of meters to 1000 m; the thickness of veins rarely exceeds 1 m. The vertical extent of ore mineralization is more than 500 m. The veins are accompanied by greisen selvages up to 0.5 m thick. Isolated linear zones, swells, and columnar bodies (Mo stocks) composed of greisen are also known. The ore-bearing quartz veins and greisen bodies are closely associated with aplite, microgranite, and kalgutite (ongonite) dikes. The intricate interrelations of kalgutite dikes with ore veins and greisen bodies indicate that they all were formed almost contemporaneously.

The evolution of the Kalguty fluid–magmatic system comprises two stages and five substages that correspond to several pulses of emplacement of magmatic melts and hydrothermal metasomatic alteration.

The first, premineral stage is related to the porphyritic biotite granite of the first intrusive phase (γ–$l\gamma T_3$–J_1kl) and includes only a tourmaline–wolframite–quartz substage.

Corresponding author: A.A. Potseluev. E-mail: poan@ign.tpu.ru

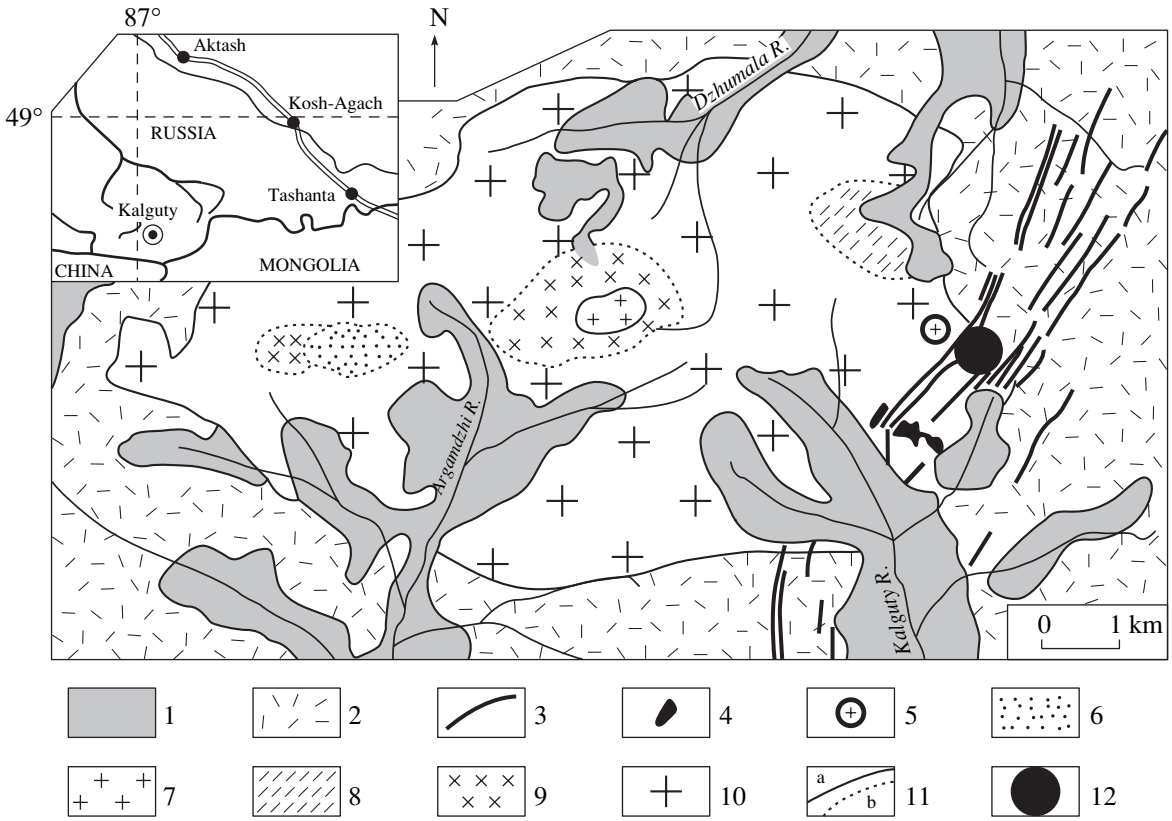

Fig. 1. Geological sketch map of the Kalguty district, modified after the data of B.G. Sementsov and I.Yu. Annikova. (1) Quaternary sediments; (2) Devonian volcanosedimentary rocks; (3–5) Early Jurassic East Kalguty Complex: (3) elvan (ongonite) dikes, (4) granite porphyry stocks, (5) greisen of Molybdenum Stock; (6–10) Late Triassic–Early Jurassic Kalguty Complex of granites and leucogranites; (11) geological boundaries: (a) intrusive, (b) facies; (12) Kalguty deposit.

The second, main stage of ore formation embraces the substage of autonomous greisen mineralization of the Mo stock type related to the emplacement of granite porphyry of the second intrusive phase ($\gamma\pi_2J_1vk$) and the subsequent rare-metal–huebnerite–quartz and sulfide–sulfosalt–quartz and final carbonate substages of mineral formation. The products of the sulfide–sulfosalt–quartz substage are mainly superimposed on the older mineral assemblages with formation of complex sulfide–sulfosalt–rare-metal–huebnerite–quartz veins, which are the main objects of this investigation. The emplacement of intermineral kalgutite ($\gamma\pi_3J_1vk$) and microgranite stocks and dikes is also related to this stage.

The deposit was formed as a result of evolution of one fluid–magmatic system (Annikova, 2001; Potseluev and Kotegov, 2003) as evidenced from isotopic and geochemical data, in particular, from correlation of normalized geochemical spectra.

The granites, intramineral kalgutite dikes, greisen bodies, and ore veins were formed 213–202 Ma ago (Vladimirov et al., 1998; Annikova et al., 2002). This time coincides with the final stage of evolution of the Siberian superplume, characterized by local occurrences of mantle ore-bearing magmatism dated at 230–210 Ma (Dobretsov, 1997, 2003).

In our opinion, the isotopic characteristics [$^{87}Sr/^{86}Sr$, $\varepsilon(Nd)_t$] of the Kalguty granite and kalgutite dikes (Vladimirov et al., 1998) testify to a mixed type of the magma source. The occurrence of kalgutites indicates that mantle-derived magma chambers were located at the base of the granitic batholith that occupies the southern Gorny Altai.

MINERALOGY AND GEOCHEMISTRY

Wolframite, molybdenite, beryl, bismuthinite, other Bi minerals, and chalcopyrite are the major ore minerals for which grades and reserves are estimated. The quartz–bismuth–molybdenum–tungsten, quartz–tungsten, quartz–tungsten–molybdenum, and autonomous greisen types of ores have been recognized at the deposit. A new type of W–Mo–Bi–Cu–Be ore hosted in wall-rock greisen zones was identified in the course of this study (Potseluev et al., 2001).

The ores consist of more than 50 hypogenic ore and gangue minerals (Table 1). Native metals (gold, bismuth, and copper) and graphite occur along with common oxides, sulfides, and sulfosalts. Quartz and muscovite are the major gangue minerals. The total amount of feldspars, fluorite, tourmaline, and other gangue miner-

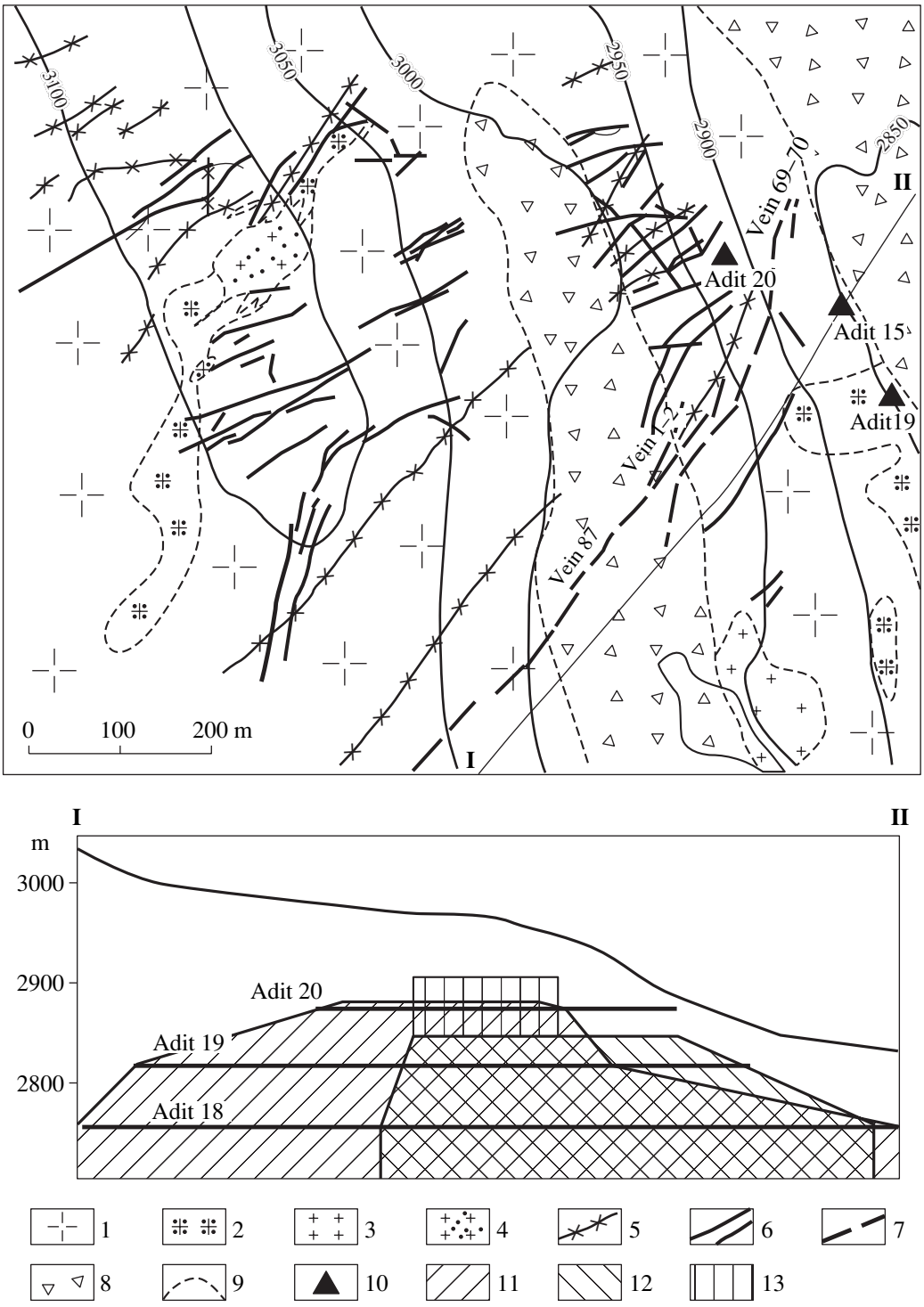

Fig. 2. Geological sketch map of the Kalguty deposit and section along line I–II with projections of the main orebodies, after the data of the Kalguty Geological Exploration Party. (1) Porphyritic granite; (2) granite porphyry; (3) microgranite; (4) greisenized granite porphyry; (5) ongonite dike; (6) ore veins exposed at the surface; (7) ore veins not exposed at the surface; (8) residual material, hillside sediments, proluvium, and glacial and alluvial sediments; (9) geological boundary; (10) adit mouth; (11) projection of Vein 87; (12) projection of Vein 69–70; (13) projection of Vein 1–2.

als does not exceed 5%. Previously unknown graphite, pavonite, gladite, lindströmite, tetradymite, and Bi-tennantite have been identified in the process of the complex evaluation of the deposit.

The oxidation zone is traceable down to 300 m from the Earth's surface (level of Adit 19, 2818 m asl). Supergene oxidation is largely developed along the tectonic zones and ore lodes. The diversity of the primary

Table 1. Mineral composition of ore from the Kalguty deposit, modified after Kryukov et al. (1986)

Mineral	Rare		Gangue minerals
	hypogenic	supergene	
Major	Huebnerite, wolframite, molybdenite, chalcopyrite, molybdenite, pyrite		Quartz
Minor	Sphalerite, tetrahedrite, emplectite, aikinite, bismuthinite, scheelite	Limonite, hematite, hydrohematite, hydrogoethite, chalcocite, bornite, covellite, azurite, malachite, cuprite	Muscovite, beryl, feldspar, tourmaline, fluorite, sericite, biotite, apatite
Rare	Native copper, native bismuth, cassiterite, ilmenite, magnetite, stannite, pyrrhotite, cubanite, galena, galenobismuthite, jamesonite, boulangerite, luzonite, tetradymite, joseite-A, rutile, molybdoscheelite, native gold, Bi-tennantite, pavonite, gladite, lindströmite, cuprobismuthite	Psilomelane, tungstite, molybdite, powellite, bismuthite, basobismuthite, bismite	Monazite, garnet, topaz, Li-bearing muscovite, calcite, siderite, ankerite, graphite

Table 2. Concentration factors and coefficients of variation of chemical elements in veins 87, 69–70, and 1–2

Concentration factor relative to the clarke value	Coefficient of variation, %				
	<50	50–70	70–100	100–200	>200
>1000				Mo, W, Bi	
100–1000	Cd			Cu, Sb, As, Sb, Ag, Pd, Pt	
10–100					Be
5–10		Cr	Cs, Au,	Zn	Pb, Os
1–5	Ge, Sn		Fe, Rb	Mn, Nb, Li, Lu, Ta, U, P	Ba
<1	Sr	K, Ni, Zr, Y, Sc	Na, Ga, Ti, V, Co, Au, Eu	V, La, Ce, Sm, Tb, Yb, Th	Na, Hf, Ba

minerals is supplemented by a rather long list of supergene minerals (Table 1). Chalcocite, covellite, azurite, malachite, limonite, and hydrohematite are the most abundant.

The distribution of 48 chemical elements, including the major ore components and all potentially valuable admixtures (including rare, rare-earth, and radioactive elements and noble metals), has been studied at the deposit (Table 2).

Many elements are characterized by high concentrations in ore veins. The concentration factors, i.e., the ratios of the measured contents to the global average concentrations of particular elements (these values are often referred to as the clarkes in the Russian literature) are as follows (numerals in parentheses): Bi (12360), W (6480), Mo (4750), Pt (450), Cd (340), Sb (290), Cu (230), Ag (200), As (133), Pd (127), Be (37), Cs (10), Pb (10), Au (9), Zn (9), Os (6.1), and Cr (5.2).

The geochemical spectra of the studied veins (nos. 87, 69–70, and 1–2) do not differ fundamentally from one another, as confirmed by the normalized curves, which practically merge into one line. The elements are connected with one another by a strong positive correlation ($\tau \geq 0.72$), which indicates their cognation.

The elements that determine the geochemical specialization of veins are characterized by an extremely nonuniform distribution (Table 2), reflected in high coefficients of variation ($V > 100\%$).

Noble metals. The special study of ore and host rocks for noble metals (Au, Ag, Pt, Pd, and Os) involved various analytical methods (Tables 3, 4).

The voltampermetric method elaborated at the Gold–Platinum Geological Analytical Center of Tomsk Polytechnical University was accepted as the basic technique. Controlling determinations of Au, Pt, and Pd were carried out with AAS at the laboratory of the Institute of Geology, Siberian Division, Russian Academy of Sciences (RAS). The Ag contents were controlled by emission spectroscopy and INAA. A comparison of the basic and controlling determinations has shown that the analytical results for Au, Ag, and Pt correspond to quantitative determinations, whereas the results for Pd should be regarded as semiquantitative determinations. No systematic discrepancy in determining Pt, Pd, and Au contents with the inversion voltampermetric method and AAS was established.

The noble metal contents in ore from the Kalguty deposit reach (ppm) 0.05 Au, 41 Ag, 3.5 Pt, 0.7 Pd, 0.09 Os, and 0.019 Rh. High noble metal contents are notable not only in orebodies but also in greisen selvages, albitized granite porphyry, and altered kalgutite dikes. The distribution of elements is extremely nonuniform; as a rule, the coefficient of variation is >100%.

Table 3. Noble metals in ore veins and metasomatically altered rocks at the Kalguty deposit

Ore veins and metasomatic rocks (number of samples)	Ag		Au		Pt		Pd		Os	
	ppm		ppb							
	average / range	*V*, %	average / range	*V*, %	average / range	*V*, %	average / range	*V*, %	average / range	*V*, %
Ore-bearing quartz veins (35)	8.4 / 0.2–41	125	17 / 0.5–50	90	449 / 0.5–3490	185	63 / 0.5–700	190	6 / 0.05–45	210
Greisen selvages (52)	1.6 / 0.06–9.4	150	15 / 0.5–55	105	259 / 0.5–4130	260	16 / 0.5–69	100	4 / 0.03–92	400
Greisenized and chloritized kalgutite dikes (6)	1.2 / 0.007–4	144	116 / 8–152	170	265 / 0.5–700	130	8 / 5–11	31	7 / 0.03–30	170
Mo stock 1 greisen body (38)	3 / 0.1–6	59	27 / 0.5–178	160	336 / 0.5–1500	120	99 / 1–640	150	5 / 0.03–14	100
Mo stock 2 greisen body (4)	0.25 / 0.15–0.4	50	14 / 1–46	150	515 / 0.5–1600	150	45 / 1–110	110	n.a.	–
Albitized granite porphyry (5)	0.1 / 0.006–0.25	83	29 / 3–84	115	802 / 150–1800	94	115 / 10–500	190	0.25 / 0.15–0.4	150
Greisenized porphyritic biotite granite (1)	0.04	–	93	–	28	–	10	–	0.8	–
Clarke value, after Taylor and McLennan (1985)	0.05		1.8		n.a.		0.5		n.a.	

Note: Here and in Tables 5 and 7, n.a. denotes not analyzed.

The albitized granite porphyry is noticeably distinguished by its Au, Pt, and Pd contents. The formation of these rocks immediately predated the formation of the rare-metal–huebnerite–quartz and sulfide–sulfosalt–quartz veins of the main ore-forming stage. The hydrothermally altered intermineral kalgutite dikes are characterized by the highest Au content. Quartz veins are also enriched in noble metals. The higher Au, Pt, and Pd contents in the altered granite porphyries and kalgutites relative to veins and greisen selvages indicate that these igneous rocks are promising for noble metal ore mineralization.

The major ore minerals (wolframite, molybdenite, chalcopyrite, pyrite, bismuthinite, etc.) are contrastingly different in noble metal contents (Table 4).

The highest Au contents, detected in graphite grains (100 ppm), are related to microinclusions of gold minerals 4–6 nm in size (Potseluev et al., 2004). The Au content in pyrite from ore veins amounts to 54 ppm and is much higher than in pyrite from the Mo stock. Gold also occurs in quartz from various rocks. Quartz from albitized granite porphyry is the most auriferous.

Gold has been detected as two species: (1) native gold of a low fineness (150–300) and with Cu and Ag as the main impurities and (2) finely dispersed gold of a high fineness (835–964) and with Ag, Cu, Hg, and Te as impurities (Fig. 3). In central parts of gold grains, the fineness is higher by 1–7 units relative to the grain margins, enriched in impurities.

In the course of ore processing, gold accumulates largely in sulfide tailings (5 ppm) of wolframite concentrate (Table 5). Silver is also left in sulfide tailings; however, its grade in wolframite and molybdenite concentrates is also rather high (67–70 ppm). The Pt grade is less differentiated; however, is relatively high in wolframite concentrate (530 ppb). A high Pd grade is also noted in wolframite concentrate (50 ppb); however, Pd accumulates to a greater extent in sulfide concentrate (103 ppb) together with gold and silver. All data indicate that gold mineralization is related to the sulfide–sulfosalt–quartz mineral assemblage.

Silver accumulates largely in sulfides and sulfosalts. The highest Ag content is established in pavonite (7.3%), cuprobismuthite (1.2%), and gladite (0.14%). A high Ag content is characteristic of graphite grains (up to 0.14%), likely owing to microinclusions of its minerals. High Ag contents are also detected in molybdenite (up to 260 ppm), chalcopyrite (up to 200 ppm), and pyrite (up to 27 ppm). Silver is the main impurity in gold of high fineness, where its content reaches 16%.

High PGE contents were revealed in pyrite (PGE sum = 760 ppb), wolframite (PGE sum = 369 ppb), and molybdenite (PGE sum = 82 ppb). The maximum Pt content was established in pyrite (670 ppb) and wolframite (313 ppb). High Pd contents ($n \times 10$ ppb) are characteristic of all three minerals. The highest Os content (1.6 ppb) was detected in molybden-

Table 4. Noble metals in minerals from the Kalguty deposit

Mineral	Material, analytical method (number of samples)		Au, ppb	Ag, ppm	Pt	Pd	Os
					ppb		
Wolframite	Vein 87, INAA (8)		25	1.1	–	–	–
	Mo stock 1, INAA (4)		25	0.5	–	–	–
	Concentrate, IVAM (1)		–	–	313	56	0.03
Molybdenite	Vein 87, INAA (5)		12	78	–	–	–
	Mo stock 1, INAA (3)		13	20	–	–	–
	Concentrate, IVAM (1)		–	–	6	75	1.6
Chalcopyrite	Vein 87, INAA (6)		15	51	–	–	–
	Mo stock 1, INAA (2)		15	35	–	–	–
	Concentrate, IVAM (1)		–	–	4	9	0.05
Pyrite	Vein 87, INAA (7)		54	11	–	–	–
	Mo stock 1, INAA (2)		15	20	–	–	–
	Concentrate, IVAM (1)		–	–	670	92	0.05
Quartz	Vein 87, INAA (9)		18	0.5	–	–	–
	Greisen selvages, INAA (9)		18	0.1	–	–	–
	Mo stock 1, INAA (6)		15	0.1	–	–	–
	Albitized granite porphyry, INAA (2)		27	0.1	–	–	–
	Host granite, INAA (1)		2.5	0.1	–	–	–
Graphite	Concentrate,	(2)	100×10^3	1400	–	–	–
Gladite	"Camebax"	(4)	–	1400	–	–	–
Cuprobismuthite		(1)	–	12000	–	–	–
Bi-tennantite		(3)	–	900	–	–	–
Bismuthite		(4)	–	8400	–	–	–
Pavonite		(3)	–	73000	–	–	–
Gold, <10 μm		(5)	911×10^6	87200	–	–	–

Note: INAA, instrumental neutron activation analysis; IVAM, inversion voltampermetric method; a dash denotes not analyzed.

Table 5. Noble metals in concentrates from the Kalguty deposit

Concentrate (number of samples)	Au	Ag	Pt	Pd	Os
	ppb	ppm	ppb		
Wolframite middling product (1)	120	280	110	93	n.a.
Wolframite concentrate (*GOST* (State Standard) *213-83*), (2)	10	67	530	50	0.03
Sulfide concentrate (6)	5030	270	150	103	n.a.
Molybdenite ore (3)	11	1.2	340	4.6	0.7
Molybdenite concentrate (*GOST* (State Standard) *212-83*) (2)	10	70	230	6.0	1.9

ite. Chalcopyrite is distinguished by the lowest PGE content.

Local laser spectral microanalysis detects Pt and Pd in grains of various minerals (Fig. 4). Analytical peaks of Pd are often recorded in bismuthinite and molybdenite grains, whereas Pd was detected only in one wolframite grain of the many tens of analyzed wolframite, molybdenite, bismuthinite, pyrite, and chalcopyrite grains. These data, along with the information on a high variability of Pt and Pd contents, allow us to suggest that these elements are contained in microinclusions that are not discernible with optical methods.

The high Au, Ag, Pt, and Pd contents in ore from the Kalguty deposit and products of ore concentrating are not an extraordinary fact. High contents of these elements have been detected in ores, concentrates, and

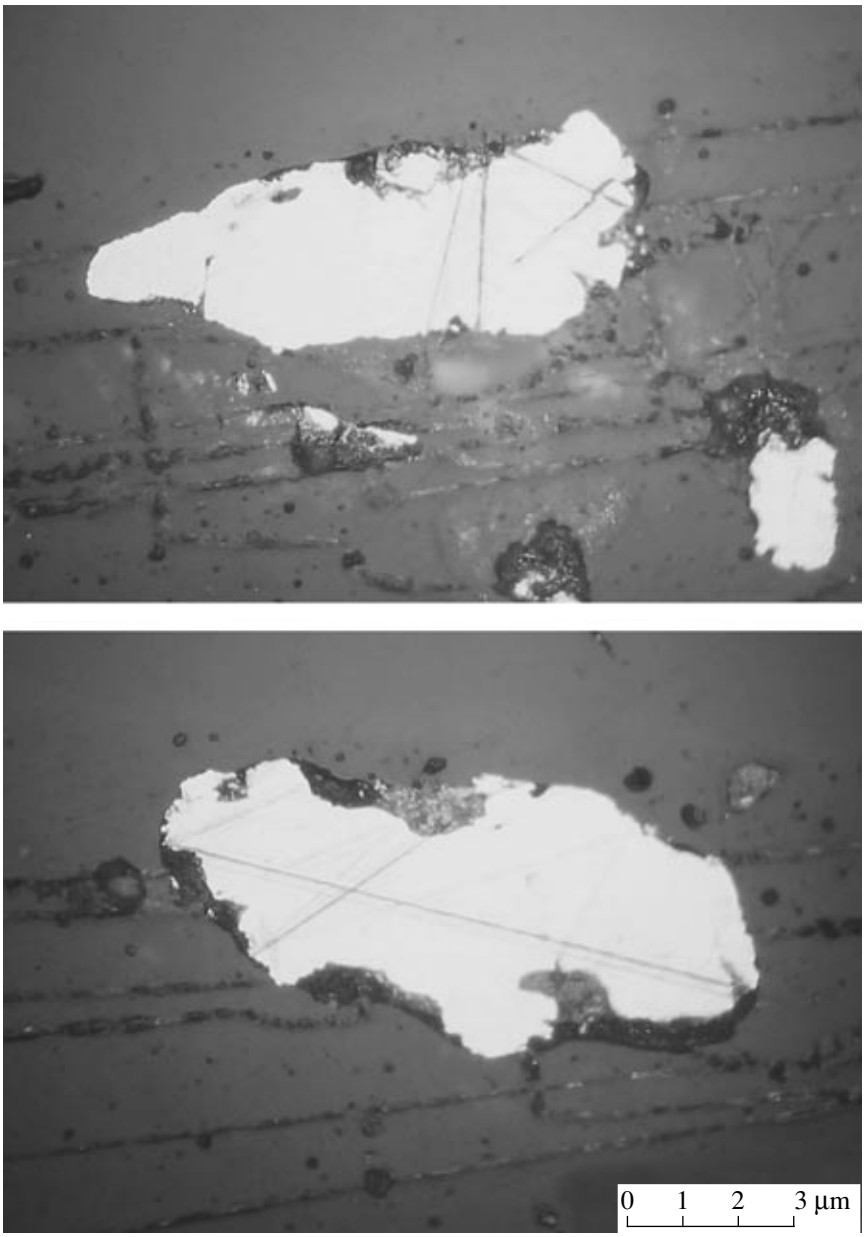

Fig. 3. Grains of native gold from ore of the Kalguty deposit. Jenavert microscope, plane reflected light.

minerals from many other postmagmatic and hydrothermal deposits, including ones related to the molybdenum–rare-metal–tungsten type (Korobeinikov, 2004; Sotnikov et al., 2001).

Contrasting zoning in the distribution of most chemical elements, including the main economic and noble metals, is observed at the Kalguty deposit (Potseluev and Kotegov, 2002). The vertical zoning of the integral vein column is represented by the following range (the coefficient of zoning is shown in parentheses): Bi (8.2), Rb (2.1)–Li (0.8)–Ag (0.5)–Au (1.8), Cu (1.5), Pt (0.6), Mo (0.11)–Pd (0.7), Cs (0.68), W (0.3), Be (0.02).

The character of zoning indicates an insignificant erosion level of the deposit and allows us to suggest that the ore mineralization extends downward below the level of Adit 18. It is expected that, with depth, the W, Mo, Pt, and Pd grades increase and the Bi, Cu, and Ag grades decrease.

The zoning of veins 87, 69–70, and 1–2 was studied in detail, especially that of Vein 87.

The range of zoning for Vein 87, the main economic vein, is based on the maxima of the average grades of each group of studied elements at the levels of adits 20, 19, and 18. The coefficient of zoning (K_z) of each element was calculated from the formula

$$K_z = C_{20}/C_{18},$$

where C_{20} and C_{18} are the average grades of an element at adit levels 20 and 18 (2872 and 2758 m asl, respec-

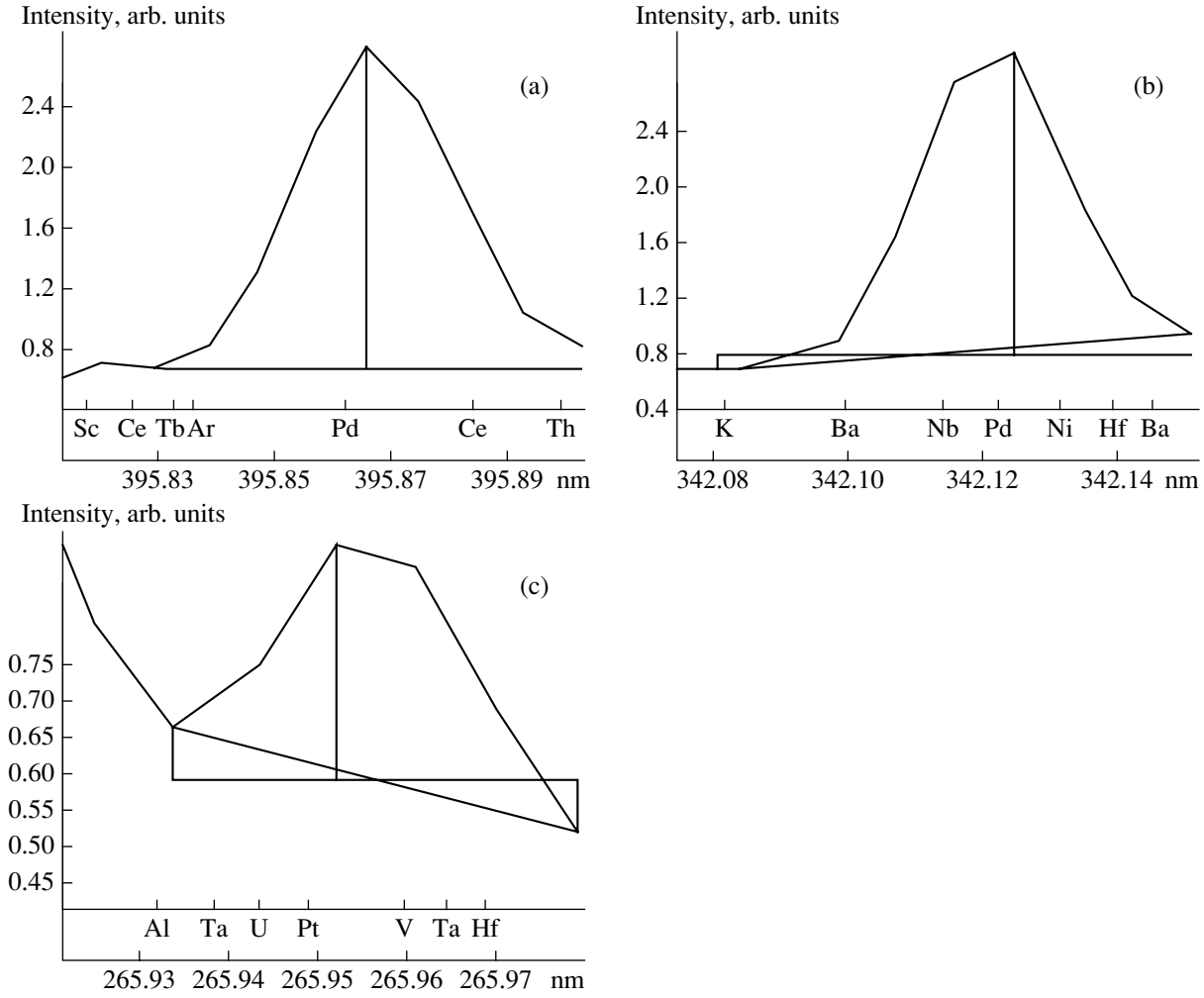

Fig. 4. Analytical peaks of Pt and Pd in (a) bismuthinite, (b) molybdenite, and (c) wolframite grains from the Kalguty deposit (results of local laser spectral microanalysis). LMA-10 microanalyzer with MAES module, analyst G.A. Babchenko, Tomsk Polytechnical University. Bismuthinite was taken from sulfide concentrate; molybdenite and wolframite, from Vein 87.

tively). The elements whose average grade in Vein 87 is lower than the clarke (the concentration factor is <1) accumulate mainly in the upper (frontal) and partially in the middle part of the vein (Table 6).

Cu and Bi are characterized by accumulation in the upper part of the ore vein, whereas the W, Be, and Mo grades increase downdip. The distribution of Au, Pt, and Pd is most likely controlled by the distribution of graphite.

Table 6. Range of axial (vertical) zoning of Vein 87

Group of elements	Concentration factor	
	>1	<1
Elements from frontal part of zoning range (level of Adit 20, 2872 m asl)	Ba (15), **Cu** (4.7), **Bi** (4.6), Li (2.4), Rb (1.9), Os (1.3), Ge (1.1), Mn (1.1)	Hf (23), La (15), Th (8), Tb (6), Sm (5), Ce (5.9), ETR (4.3), Na (3.2), Ti (2.5), V (1.9), Sc (1.8), K (1.8), Eu (1.6), Zr (1.4), Co (1.4), Sr (1.1)
Elements from middle part of zoning range (level of Adit 19, 2812 m asl)	Fe (2), **Au** (1.6), Sn (1.2), **Pt** (0.6), Sb (0.4), **Ag** (0.3), Zn (0.3), Pb (0.2)	Ni (1.8), Yb (1.5), Ga (1.3), Y (1), Cr (1)
Elements from back part of zoning range (level of Adit 18, 2758 m asl)	P (0.73), Cs (0.7), **W** (0.68), Lu (0.5), U (0.4), C (0.4), **Be** (0.39), Nb (0.36), Ta (0.3), **Pd** (0.22), **Mo** (0.08)	–

Note: Numerals in parentheses are coefficients of zoning; the major ore elements and the most valuable admixtures are boldfaced.

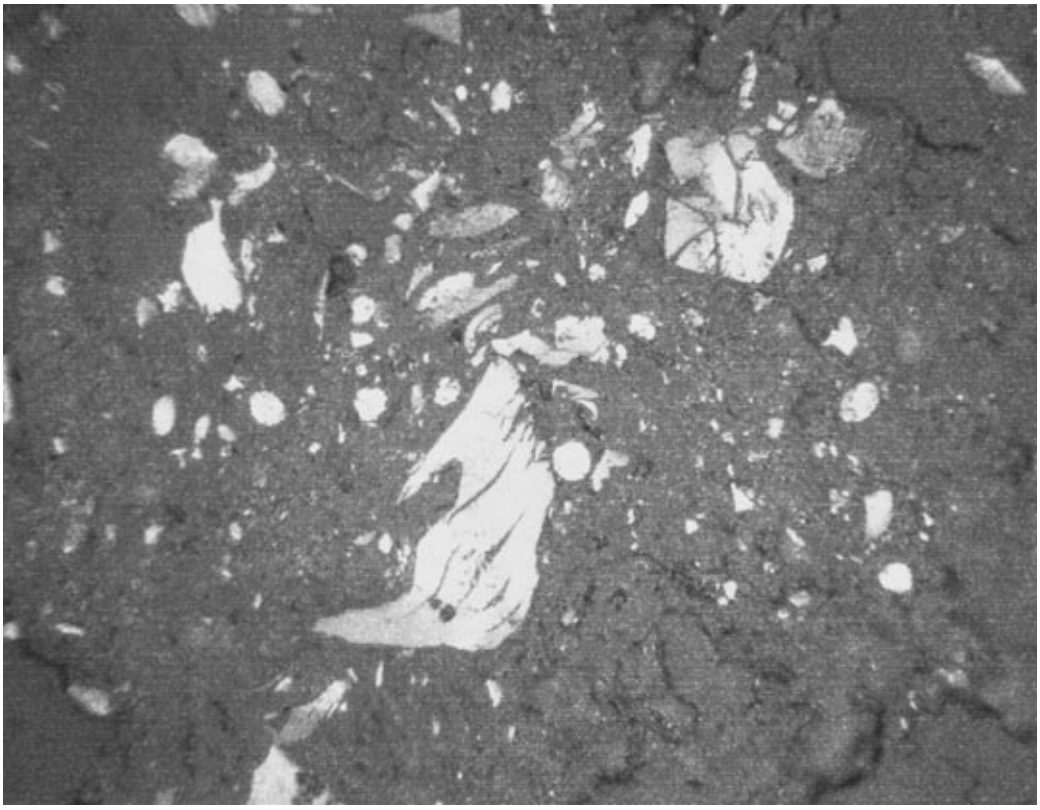

Fig. 5. Graphite grains (light) intergrown with quartz (gray). Jenavert microscope, plane reflected light, magn. 250.

The REE pattern based on the INAA results is rather differentiated. LREE are selectively accumulated in the upper (frontal) part of the vein, while HREE concentrate in the lower (back) part. The REE differentiation reflects the accumulation of monazite as the main mineral concentrator of LREE in the upper part of the vein, whereas Lu largely concentrates in wolframite, whose content increases with depth (Potseluev et al., 2002).

The established range of zoning is broadly consistent with the ranges of zoning at other greisen deposits. The proportions of elements, noble metals included, in veins and greisen selvages also demonstrate a regular trend. In general, the segments of veins with the highest noble metal contents are accompanied by greisen selvages depleted in these elements and vice versa (Potseluev and Kotegov, 2002). These relationships testify to the genetic cognation of veins and greisenization of wall rocks. The observed difference in the character of geochemical zoning in veins and greisen selvages may be caused by substantially distinct mechanisms and conditions of migration and deposition in open fissures, on the one hand, and in zones of metasomatic alteration of wall rocks, on the other hand.

Graphite grains (<0.5 mm) occur as intergrowths with quartz and sulfides (Fig. 5). The graphite grains themselves contain inclusions and microveinlets of chalcopyrite, pyrite, bismuthinite, and Bi-tennantite. The results of mineralogical and detailed geochemical studies show that graphite belongs to the late sphalerite–molybdenite–chalcopyrite–quartz and sulfosalt mineral assemblages, which were deposited at the sulfide–sulfosalt–quartz substage of the second (main) stage of mineral formation.

The Raman spectra of two graphite grains in the region of intense oscillations of C–C bonds are represented by lines of complex configuration that markedly differ from the spectrum of typical crystals of pyrolytic graphite (Fig. 6). The Raman spectra of the studied graphite do not reproduce a distinctly expressed narrow peak of 1580 cm^{-1} of graphite monocrystals and only mimic its spectral characteristics as wide peaks with centers at 1350 cm^{-1} (the D band) and 1590 cm^{-1} (the G band). These spectra are typical of the disordered, polycrystalline material transitional to holocrystalline graphite. The spectrum of the first grain corresponds to a more amorphous state, and the spectrum of the second grain, to a more crystalline state.

The size of graphite microcrystals estimated from relationships of integral spectrum intensities at 1350 and 1580 cm^{-1} and the crystal dimensions assessed with X-ray diffraction (Dresselhaus et al., 2000) is 4–6 nm.

The D and G Raman spectral bands in the studied samples have different intensities and half-widths. The displacement toward 1590 cm^{-1} and appreciable widening of the main, G band may be caused by occurrence

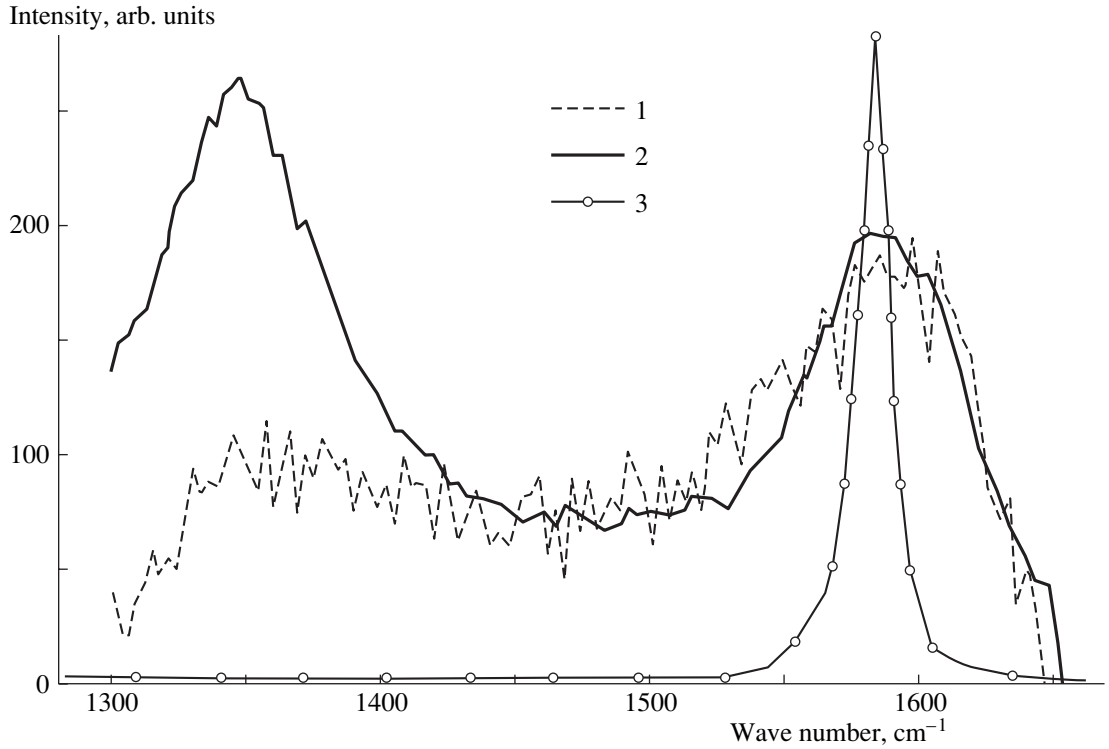

Fig. 6. Raman spectra of graphite from the Kalguty deposit. Ramanor U1000 spectrometer, analyst A.P. Shabanin, United Institute of Geology, Geophysics, and Mineralogy, Siberian Division, RAS. (1, 2) Graphite grains; (3) reference sample of pyrolytic graphite crystal.

of disordered structures arising as a result of incorporation of various ions between graphite layers (McCulloch et al., 1995).

The carbon content in noncarbonate species and its spatial distribution were determined by coulometric titration of trench samples. The average C content in samples is 0.035 ± 0.01%, which is much higher than the global average (0.02%); the range is 0.02–0.12%. The C content in the vein increases with depth from 0.025% at the upper level to 0.049% at the lower level.

The carbon distribution within Vein 87 has a regular character (Fig. 7). Its content increases from the upper and marginal parts of the vein downward and to the central portion. The samples enriched in Pt are localized near the contour line of 0.03% C, while the zone enriched in gold (>20 ppm) occurs as a cap above the contour line of 0.08% C.

High Au, Ag, Hg, Te, Sb, Bi, Cu, Pb, Zn, Fe, and S contents were established in graphite grains (Table 7). It should be emphasized that Cu, Bi, and S are the major ore components, and their contents in graphite are close to the average grade in ore. The contents of other elements (except Fe) in graphite are one to two orders of magnitude higher than their grades in ore; this is especially typical of Au and Ag.

The geochemical spectrum of the minerals included in graphite (the so-called graphite assemblage) significantly differs from the spectrum of the minerals belonging to the earlier assemblage. Higher Ag and lower Sb contents are characteristic of the minerals related to the graphite assemblage.

The high contents of the aforementioned elements in graphite grains may be caused by microinclusions of their minerals; by analogy with graphite, the dimensions of microcrystals may be $n \times 1$ nm. First of all, this concerns Cu, Bi, and S. As follows from the results of Raman spectroscopy, disordered structures that arose owing to incorporation of various ions may occur between graphite layers, and Au, Ag, Hg, and Te may be among these ions.

According to measurements on a Delta mass spectrometer at the United Institute of Geology, Geophysics, and Mineralogy, Siberian Division, RAS (analyst V.A. Ponomarchuk), graphite is characterized by enrichment in the light isotope ^{12}C. The $\delta^{13}C$ value varies within a narrow range from –26.3 ± 0.4 to –26.6 ± 0.3‰. These isotope ratios are typical mainly of reduced carbon species (Faure, 1986), graphite being an example. At the same time, the enrichment in a light isotope may be a result of a high degree of fractionation of matter during the transport of deep fluid in the zone of ore formation.

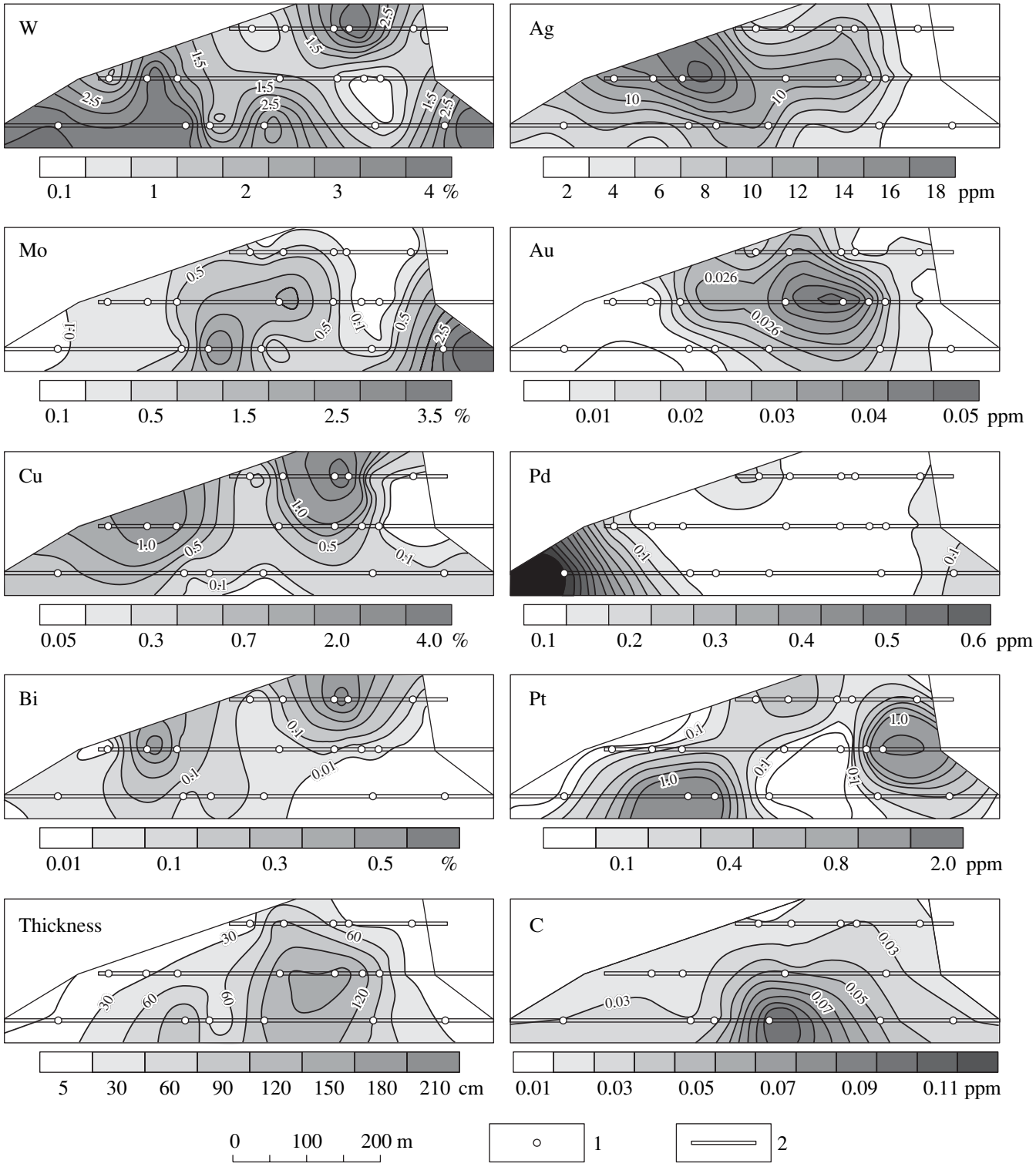

Fig. 7. Distribution of carbon, noble metals, and main ore components in Vein 87 (projection on the vertical plane). (1) Sample location; (2) adit levels.

FLUID INCLUSION STUDY

The study of fluid inclusions in ore-bearing quartz that was performed gave information on the fluid composition and its spatiotemporal variation. Monomineral quartz fractions were investigated with gas chromatography on an LKhM-80 device (analyst L.N. Fomina) at the Laboratory of Thermobarogeochemistry of the Institute of Mineralogy and Petrography, Siberian Divi-

Table 7. Average chemical compositions of minerals (Camebax microprobe results, analyst O.S. Khmel'nikova, United Institute of Geology, Geophysics, and Mineralogy, Siberian Division, RAS), wt %

Mineral		Bi	Cu	Pb	Fe	Zn	Ag	Sb	Te	S	Au	Hg
Graphite		1.95	1.05	0.29	0.35	0.19	0.08	0.14	0.20	2.07	0.01	0.01
Inclusions in graphite	Bi-tennantite	63.8	13.2	0.26	0.48	0.16	0.74	0.03	<0.01	19.0	<0.01	<0.01
	Bismuthinite	79.6	0.50	0.12	<0.01	<0.01	0.88	<0.01	0.05	17.5	<0.01	<0.01
	Chalcopyrite	0.04	34.2	<0.01	30.3	0.10	0.05	n.a.	0.01	34.8	<0.01	<0.01
Minerals of earlier assemblage	Bi-tennantite	39.0	24.3	<0.01	0.77	3.65	0.09	10.3	0.01	21.5	<0.01	<0.01
	Bismuthinite	77.5	0.67	3.05	<0.01	0.01	0.08	0.04	0.01	18.2	<0.01	<0.01
	Chalcopyrite	0.07	33.7	<0.01	31.3	0.1	<0.01	0.06	0.1	35.1	<0.01	<0.01
Ore vein*		0.11	0.58	0.01	4.9	0.04	0.001	0.003	n.a.	2.53	15×10^{-7}	n.a.

* The content of elements in the vein was determined from the analysis of trench samples.

sion, RAS, in Novosibirsk. H_2O, CO_2, CO, H_2, and N_2, as well as saturated (CH_4, C_2H_6, C_3H_8, C_4H_{10}, C_5H_{12}, and C_6H_{14}) and unsaturated (C_2H_2 and C_2H_4) hydrocarbons (Table 8), were analyzed.

Fluid inclusions were studied in plates 0.2 mm thick polished on both sides. About 100 inclusions were studied in total.

The main types of inclusions are shown in Fig. 8. By morphology and composition, they are classified into primary (xenogenic and authigenic) inclusions (Figs. 8a–8c) and secondary inclusions (Fig. 8d). Two-phase inclusions are predominant, single-phase inclusions (gas or liquid) are less abundant, and three-phase inclusions are rare. The liquid phase is represented by water with some amount of dissolved salts (up to 24 wt % NaCl equiv). The solid phases consist of salt crystals and ore minerals, while the gas phase is composed mainly of CO_2 and some other gases.

The homogenization temperature of fluid inclusions ranges from 290–340 to 140–160°C (the lowest forma-

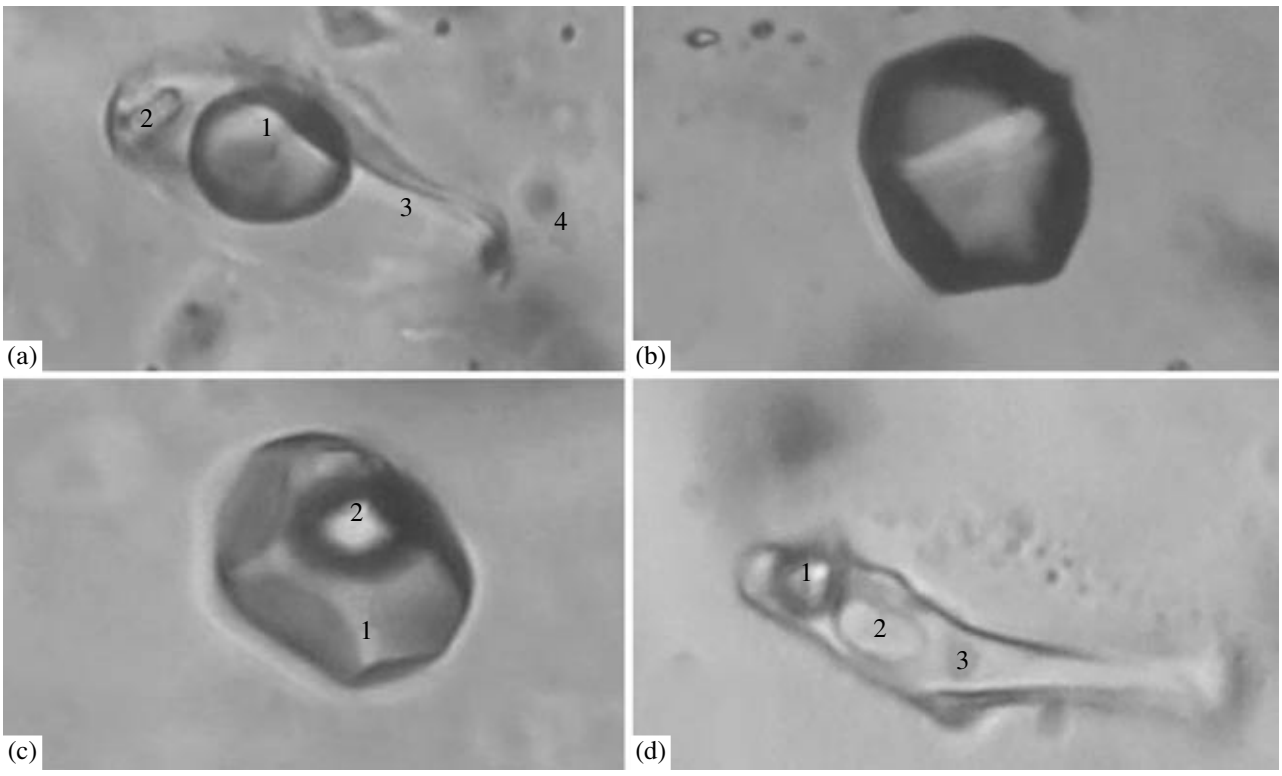

Fig. 8. Types of fluid inclusions captured by quartz. (a) Three-phase inclusion: (1) CO_2 bubble, (2) salt crystal, (3) water, (4) ore matter; (b) inclusion with a large CO_2 bubble; (c) two-phase inclusion: (1) liquid (H_2O), (2) gas bubble (CO_2); (d) three-phase inclusion: (1) CO_2 bubble, (2) salt crystal, (3) water. The size of inclusions is 20–35 μm.

Table 8. Concentrations of water and main gases in quartz from orebodies at the Kalguty deposit, mg/kg

Orebody (number of samples)		H_2O	CO_2	CO	H_2	CH_4	C_2H_2	$C_2H_{4,6}$	C_3H_8	C_4H_{10}	C_5H_{12}	C_6H_{14}	Sum of gases + H_2O
Vein 87	Level 20 (3)	1280 ± 110 1200–1600	80 ± 7 70–100	15 ± 3 10–20	<2	9 ± 0.6 8–10	7 ± 0.6 6–8	0.8 ± 0.1 0.6–1	6 ± 1 4–8	5.5 ± 1.5 4–10	3 ± 1 2–6	0.7 ± 0.1 0.4–1	1400 ± 130
	Level 19 (10)	950 ± 180 14–1600	68 ± 6.2 30–90	10 ± 2 5–20	<2	6 ± 0.4 4–8	5 ± 0.4 4–6	0.7 ± 0.1 0.4–1	5 ± 0.5 4–8	4 ± 0.5 2–6	1.6 ± 0.4 1–4	0.4 ± 0.1 0.1–0.8	1050 ± 190
	Level 18 (7)	970 ± 140 420–1400	71 ± 12 20–120	27 ± 8.7 3–60	2 ± 0.7 1–5	10 ± 2.6 4–20	6.9 ± 1.3 2–10	1.7 ± 0.6 0.6–4	9 ± 2 4–20	7 ± 1.1 4–10	3.7 ± 1.1 1–8	1.7 ± 0.5 0.2–4	1110 ± 180
	Entire vein (20)	1030 ± 100 14–1600	72 ± 5 20–120	17.5 ± 4 3–60	<2	8.2 ± 1 4–20	6 ± 0.5 2–10	1.1 ± 0.2 0.4–4	6.7 ± 0.9 4–20	5.5 ± 0.6 2–10	2.7 ± 0.5 1–8	1 ± 0.2 0.1–4	1150 ± 110
Vein 69–70	Level 19 (3)	1300 1300–1300	43 ± 12 20–60	4.7 ± 0.7 4–6	<2	3.3 ± 1.3 2–6	2.7 ± 0.7 2–4	0.3 ± 0.1 0.2–0.6	2.7 ± 0.7 2–4	2.7 ± 0.7 2–4	1 1–1	0.2 ± 0.1 0.1–0.4	1360 ± 16
	Level 18 (3)	1000 ± 150 710–1200	43 ± 3 40–50	9.3 ± 0.7 8–10	<2	5.3 ± 0.7 4–6	4 4–4	0.3 ± 0.1 0.2–0.4	4 4–4	4.7 ± 0.7 4–6	1.7 ± 0.3 1–2	0.4 ± 0.1 0.1–0.6	1080 ± 160
	Entire vein (6)	1150 ± 90 710–1300	43 ± 6 20–60	7 ± 1 4–10	<2	4.3 ± 0.8 2–6	3.3 ± 0.4 2–4	0.3 ± 0.1 0.2–0.6	3 ± 0.4 2–4	3.7 ± 0.6 2–6	1.3 ± 0.2 1–2	0.3 ± 0.1 0.1–0.6	1220 ± 100
Vein 1–2, level 20 (3)		1500 ± 120 1300–1700	60 ± 6 50–70	16 ± 4 8–20	<2	7.3 ± 1.8 4–10	6.7 ± 1.3 4–8	0.7 ± 0.1 0.4–0.8	5 ± 1.8 2–8	6 ± 2 2–10	1.7 ± 0.3 1–2	0.5 ± 0.1 0.4–0.6	1600 ± 130
Mo stock 1	Level 19 (4)	1650 ± 130 1300–1900	75 ± 13 50–110	10 ± 4 4–20	<2	5.5 ± 1.7 2–10	5 ± 1.7 2–10	0.6 ± 0.1 0.2–0.8	5 ± 1.7 2–10	5.5 ± 1.7 2–10	1.5 ± 0.3 0.8–2	0.4 ± 0.2 0.1–1	1760 ± 160
	Level 18 (6)	1420 ± 180 820–1900	77 ± 14 30–130	10 ± 2 6–20	<2	8 ± 1.3 4–10	7 ± 1 4–10	1 ± 0.3 0.4–2	6 ± 1 2–8	6 ± 1 2–8	2 ± 0.5 0–4	0.6 ± 0.1 0.1–1	1540 ± 200
	Entire stock (10)	1500 ± 120 820–1900	76 ± 10 30–130	10 ± 2 4–20	<2	7 ± 1 2–10	6 ± 1 2–10	0.7 ± 0.2 0.2–2	5.6 ± 1 2–10	6 ± 0.8 2–10	1.8 ± 0.3 0.8–4	0.5 ± 0.1 0.1–1	1630 ± 140
Mo stock 2, Earth's surface (4)		880 ± 110 570–1100	85 ± 10 60–110	43 ± 10 20–70	6 ± 0.6 5–8	15 ± 3 10–20	12.5 ± 2.5 10–20	2 ± 0.7 1–4	9.5 ± 0.5 8–10	8.5 ± 1 6–10	5 ± 0.6 4–6	1.5 ± 0.3 1–2	1070 ± 140

Note: The numerator is the average content of the component and the standard deviation; the denominator is the range. The thermal method of opening fluid inclusions at 600°C was used.

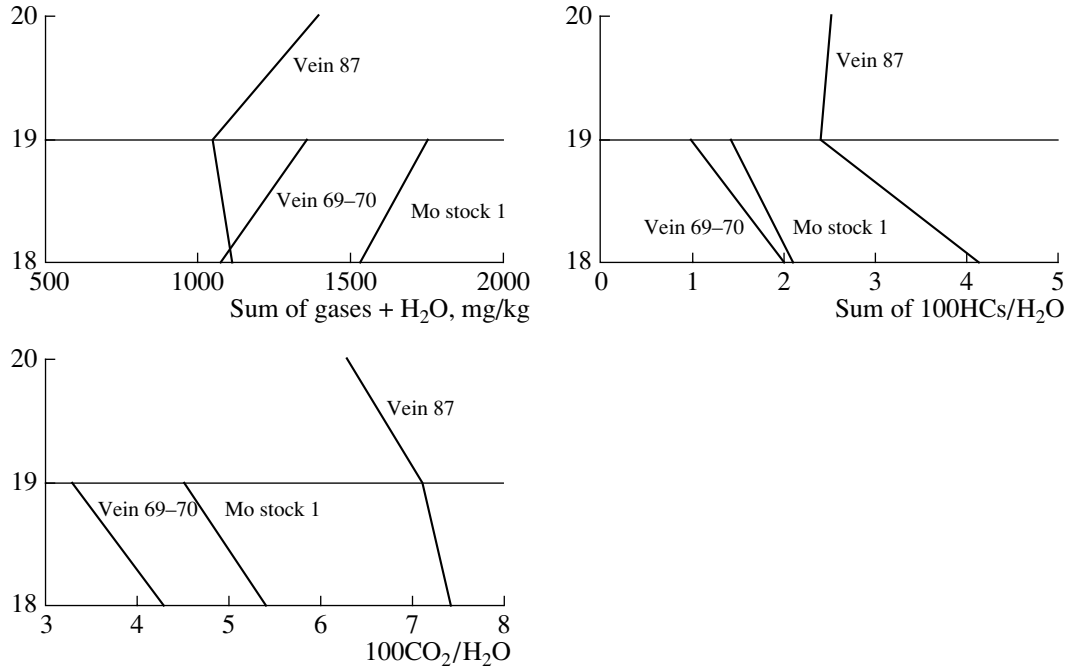

Fig. 9. Gases in quartz from orebodies at the Kalguty deposit: quantitative and compositional variations with depth (adit levels 18–20).

tion temperatures of primary and secondary inclusions, respectively). The considerable scatter of temperatures is a result of different origin of the inclusions.

Thus, the temperature of quartz crystallization at the second (main) stage was 290–340°C at a minimum. The subsequent hydrothermal alteration occurred at a lower temperature (140–160°C). Secondary inclusions were formed by sealing of fractures in quartz. The obtained temperature of the second (main) stage of mineral formation is broadly consistent with data previously reported from the Kalguty and other rare-metal greisen deposits of the Gorny Altai (Sotnikov and Nikitina, 1971; Dergachev and Nikitina, 1983; Kuzhel'naya and Dergachev, 1990).

Cryometric results on two-phase inclusions (liquid H_2O and gaseous CO_2) in quartz from Vein 87 showed that the eutectic temperature is –(24–26)°C in a first inclusion and –(25–28)°C in a second inclusion. Taking into account the temperature of ice melting (–7.5 and –(8.0–9.5)°C), the salt concentration in the liquid phase was calculated to be 11.6 and 12.5–14.0 wt % NaCl equiv.

The main components of fluid inclusions in quartz are water (up to 92%) and carbon dioxide (up to 8%); other components are detected in much lesser concentrations (Table 7).

The orebodies appreciably differ from one another in sum of gases and water. Quartz from the Mo stock 1 greisen body and Vein 1–2 is the most fluid-saturated (1630 and 1600 mg/kg, respectively); in quartz from other orebodies, the fluid concentration drops to 1050–1220 mg/kg.

As can be seen from the data obtained (Fig. 9, Table 7), this difference is primarily caused by nonuniform coverage of orebodies in the vertical direction. In general, the fluid saturation of quartz diminishes with depth. The fluid concentration in quartz decreases with depth by 58 mg/kg in Vein 87 (between adit levels 19 and 20), 47 mg/kg in Vein 69–70, and 37 mg/kg in Mo stock 1 for a depth difference of 10 m. However, the fluid concentration in quartz of Vein 87 increases from adit level 19 to level 18, this being the only exception. Taking into account previously obtained data on the ore mineralization zoning (Kuzhel'naya and Dergachev, 1990), a stagelike (wavelike) distribution of ore mineralization in Vein 87 (the main ore vein) may be supposed, so that the resource potential of this vein at deeper levels looks highly promising.

The water content in quartz from orebodies varies from 880 to 1500 mg/kg. The highest water contents against the background of other orebodies are inherent to Mo stock 1 and Vein 1–2, where its average content amounts to 1500 mg/kg. Mo stock 2 is distinguished by the lowest water content (880 mg/kg).

In all studied orebodies, the water concentration in quartz falls with depth. At the same time, in Vein 87, the concentration of water and gases in quartz markedly increases from level 19 to level 18, which is located deeper (Fig. 9).

A similar tendency toward a decrease in water content and sum of gases with depth has been pointed out for other tungsten deposits of the Gorny Altai formed at different depths (Kuzhel'naya and Dergachev, 1990).

Table 9. Variations in $100CO_2/H_2O$ ratio, hydrogen factor (K_{H_2}), and coefficient of fluid reduction (K_r) in quartz

Orebody		$100CO_2/H_2O$	K_{H_2}	K_r
Vein 87	Level 20	6.3	13.8	3.5
	Level 19	7.1	12.5	3.3
	Level 18	7.4	10.3	6.6
	Entire vein	6.9	11.9	4.5
Vein 69–70	Level 19	3.3	27.4	1.3
	Level 18	4.3	19.4	2.8
	Entire vein	3.8	23.2	2.0
Vein 1–2, level 20		4	20.1	2.8
Mo stock 1	Level 19	4.5	19.7	1.9
	Level 18	5.4	16.7	2.7
	Entire stock	5	17.9	2.4
Mo stock 2, Earth's surface		9.6	7.4	10.6

Note: $K_{H_2} = (H_2 + H_2O + HC_{total})/(CO + CO_2)$; $K_r = 100(H_2 + CO + HC_{total})/(CO_2 + H_2O)$.

This relationship is retained on various scales, from particular orebodies to ore fields.

The carbon dioxide content in quartz varies from 43 to 85 mg/kg. The CO concentrations vary from 7 to 43 mg/kg. The highest CO_2 concentrations were established in Mo stock 2 and the lowest concentrations, in Vein 69–70.

No appreciable variation in CO_2 content with depth was observed. However, the considerable decrease in water content with depth results in a markedly increasing $100CO_2/H_2O$ ratio (Fig. 9). The gradient of this parameter calculated for a depth difference of 10 m increases similarly in all orebodies from level 19 to level 20: 0.13 in Vein 87, 0.17 in Vein 69–70, and 0.15 in Mo stock 1. In Vein 87, this ratio decreases at a greater depth.

Our data are broadly consistent with the estimations previously obtained by Dergachev and Nikitina (1983) for the water and CO_2 contents and $100CO_2/H_2O$ ratio in quartz from the Kalguty deposit and other deposits of the Gorny Altai. These authors concluded that the above ratio markedly decreases from the early greisen stage of ore formation to the subsequent vein of the productive stage from 20–50 to 2–10. However, our data do not confirm the difference in this parameter between greisen of Mo stock 1 and productive quartz veins (Table 8) if the variation in the $100CO_2/H_2O$ ratio with depth is taken into account.

Hydrogen was detected in significant concentrations (5–8 mg/kg) in quartz from Mo stock 2. At the upper levels of Vein 87, the H_2 content in quartz is below the detection limit, but it increases to 5 mg/kg at the lowermost level.

Among *HCs*, methane is the most abundant; the abundances of other HCs decrease in the following order: C_2H_2, C_3H_8, C_4H_{10}, C_5H_{12}, $C_4H_{4,6}$, and C_6H_{14}. The highest HC contents were established in quartz from Mo stock 2. The HC contents in quartz increase with depth, and the general tendency to depletion in water with depth makes the HC/H_2O ratio still higher (Fig. 9).

The orebodies at the deposit significantly differ in the parameters $100CO_2/H_2O$, hydrogen factor $K_{H_2} = (H_2 + H_2O + HC_{total})/(CO + CO_2)$, and coefficient of fluid reduction $K_r = 100(H_2 + CO + HC_{total})/(CO_2 + H_2O)$.

The average $100CO_2/H_2O$ ratio varies from 3.8 in Vein 69–70 to 9.6 in Mo stock 2. Dergachev and Nikitina (1983) estimated this parameter as 4.4 for the Kalguty deposit as a whole. Our data indicate that the average values for deposits may be rather controversial if they are not tied to specific orebodies. The $100CO_2/H_2O$ ratio increases by 20–30% with depth owing to the depletion of fluid in water. Taking into account this trend, the statement on a regular increase in this ratio from the hypabyssal tungsten deposits of the Gorny Altai (the Kalguty deposit) through the mesoabyssal deposits (Kokkol and Chindagatui) to the abyssal deposits (Buguzun) (Kuzhel'naya and Dergachev, 1990) is not sufficiently substantiated because it does not take into consideration the variation in this parameter within particular deposits.

The hydrogen factor (K_{H_2}) varies from 7.4 in Mo stock 2 to 23.2 in Vein 69–70. The K_{H_2} value regularly decreases with depth in all studied orebodies. The sum in the numerator of this ratio includes HCs, and thus K_{H_2} increases at the expense of carbon that is contained in HCs. The real proportion of hydrogen and carbon in the fluid is exemplified in Vein 87 (Table 9): 2.7 at the upper level and 1.8 at the lower level, decreasing, on the whole, by 33% in the studied depth interval.

The coefficient of fluid reduction (K_r) is estimated as the ratio of the sum of reduced gases to the sum of oxidized gases. In the studied samples, this coefficient varies from 2 in Vein 69–70 to 10.6 in Mo stock 2. In all orebodies, the degree of fluid reduction increases markedly with depth.

The data obtained allow us to estimate the compositional variation of fluid in quartz as a projection on the plane of Vein 87 (Fig. 10). Analysis of the variations in gas and water concentrations and their proportions together with the variations in vein thickness and graphite content indicates that these parameters are interrelated and demonstrates a combination of longitudinal and vertical zoning. On the vertical projection of Vein 87, the CO_2 concentration increases toward the vein center and with depth.

In the center of Vein 87 at its middle level, where the thickness of the vein is maximal, an anomalously low water content is observed. The saturation with fluid

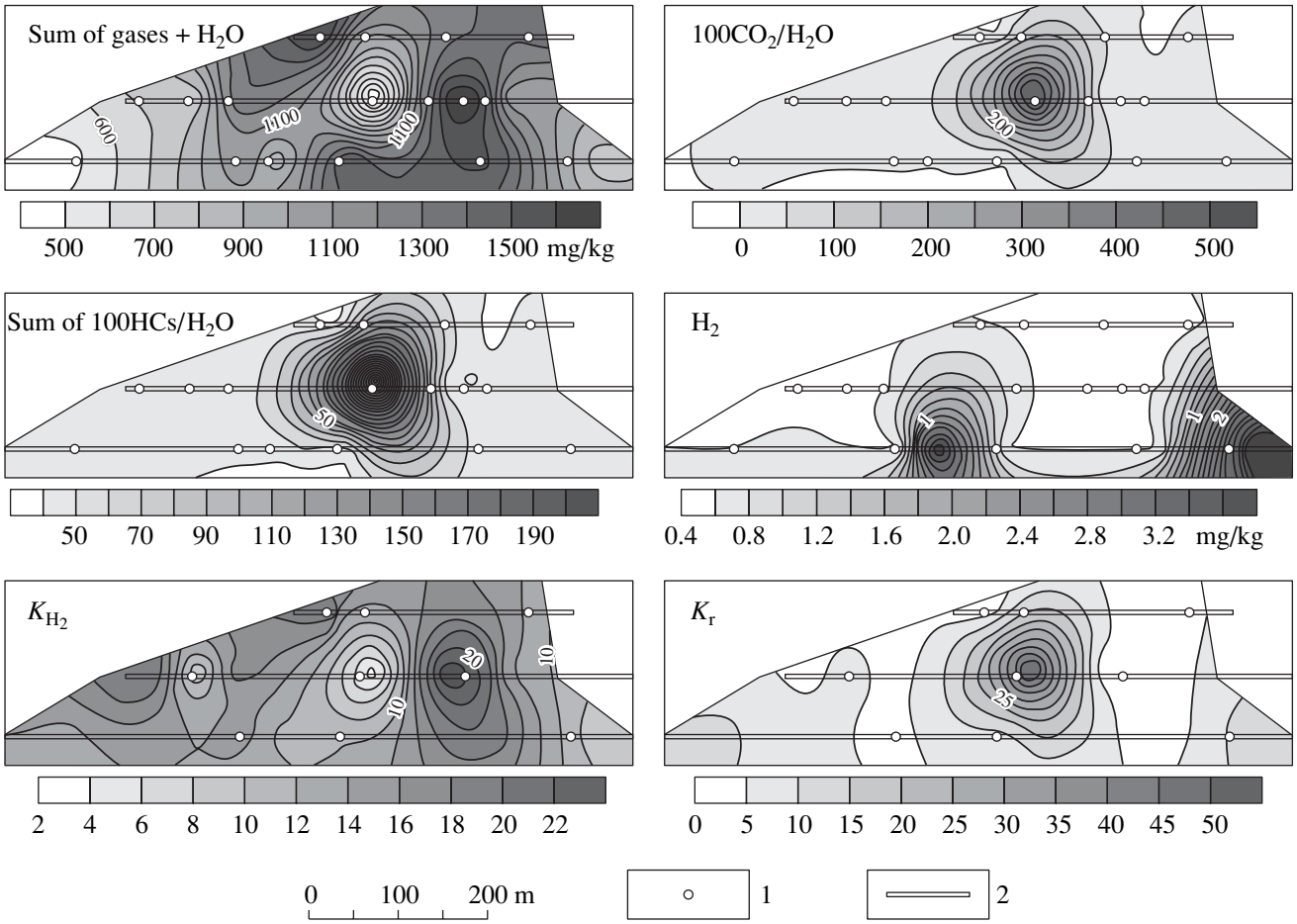

Fig. 10. Composition of fluid inclusions in quartz and thickness of Vein 87: variations in the projection on the vertical plane. (1) Sample location; (2) adit levels.

increases from the frontal zone toward the center and from the upper level downward.

The variation in composition of fluid inclusions is related to the variable concentrations of oxygen, hydrogen, and carbon. The water and gas contents in quartz from Vein 87 at the upper and lower levels were recalculated to the contents of chemical elements (Table 10). The consideration of these data reveals a general pattern of compositional variation of the ore-forming fluid in the process of its migration to the zone of ore deposition.

The updip transport of the fluid for 120 m is accompanied by an increase in oxygen concentration by 29% owing to its contents in oxidized species (H_2O and CO_2). The content of oxygen bound in CO decreases by 44%. The hydrogen content increases by 26% at the expense of oxidized species (H_2O) and decreases by 40% at the expense of reduced species (H_2 + HCs).

Table 10. Elemental composition of gases from quartz in Vein 87, ppm

Level	Oxygen			Hydrogen		Carbon		
	Species							
	H_2O	CO_2	CO	H_2O	H_2 + HCs	CO_2	CO	HCs
20 (upper)	1133 (+31.4%)	58 (+11.5%)	8.6 (–44%)	142 (+31.4%)	5.6 (–40%)	21.8 (+12%)	6.4 (–45%)	26.3 (–20%)
	Σ1200 (+29%)			Σ147.6 (+26%)		Σ54.5 (–15%)		
18 (lower)	863	52	15.4	108	9.2	19.5	11.6	33
	Σ930.4			Σ117.2		Σ64.1		

Note: Numerals in parentheses are variations (%) in element contents from the lower level to the upper level.

While the oxygen and hydrogen contents increase up the dip of orebody, the carbon content decreases by 15% (9.6 mg/kg). The percentage of carbon contained in reduced species (HCs and CO) markedly falls and is not balanced by a slight increase in CO_2 content. The loss of carbon from fluid amounts to 9.6 mg/kg. It is evident that a part of C previously contained in fluid was fixed in graphite.

Taking into account that the average graphite content in the vein is 0.035 wt % (350 mg/kg), it is possible to estimate the amount of fluid consumed for accumulation of the detected amount of graphite. Having divided the graphite content in the vein (350 mg/kg) by the quantity of carbon released from fluid (9.6 mg/kg) and multiplied by the total concentration of fluid in quartz (1110 mg/kg at level 18), we obtain 40.5 g of fluid per kilogram of quartz.

Undoubtedly, these estimates are only tentative because they have been made with several assumptions. However, the occurrence of graphite in the veins is consistent with the established compositional variations in fluid inclusions in quartz and thus emphasizes once again the genetic links between these phenomena.

Thus, the appearance of graphite in veins testifies to an abrupt change in composition of the fluid phase. It is difficult to ascertain which parameters or their combinations (*P*, *T*, *X*, etc.) exerted the greatest effect on carbon binding in graphite. It is evident that the main prerequisite for the formation of graphite was occurrence of HCs and a limited supply of oxygen insufficient for complete oxidation of all components.

The data obtained testify to the active participation of HCs and hydrogen in the ore formation at the Kalguty deposit. As a result, graphite arose in the ore as a regularly distributed solid phase. Taking into consideration the geochemical attributes of graphite, it may be concluded that deep metalliferous reduced fluids served as a source of noble metals.

CONCLUSIONS

(1) The ore at the deposit consists of more than 50 hypogenic ore and gangue minerals. Native gold, bismuth, copper, and carbon in the form of graphite occur here along with abundant oxides, sulfides, and sulfosalts.

Graphite is characterized by a disordered, polycrystalline state transitional to the holocrystalline state. The carbon isotopic composition of graphite is distinguished by enrichment in a light isotope. $\delta^{13}C$ varies in a narrow range from -26.3 ± 0.4 to $-26 \pm 0.3‰$.

Graphite grains show high concentrations of many chemical elements, including Au and Ag, probably, due to microinclusions of minerals of these elements.

(2) Ore veins at the deposit are distinguished by high contents of many chemical elements. The concentration factors are as follows (numerals in parentheses): Bi (12360), W (6480), Mo (4750), Pt (450), Cd (340), Sb (290), Cu (230), Ag (200), As (133), Pd (127), Be (37), Cs (10), Pb (10), Au (9), Zn (9), Os (6.1), and Cr (5.2). The geochemical spectra of the studied veins (87, 69–70, and 1–2) do not differ fundamentally from one another.

The elements that determine the geochemical specialization of veins are characterized by an extremely nonuniform distribution, reflected in high values of the coefficient of variation ($V > 100\%$).

(3) The orebodies and metasomatically altered rocks at the Kalguty deposit are characterized by high contents of noble metals, reaching 116 ppb Au, 8.4 ppm Ag, 802 ppb Pt, 115 ppb Pd, and 7 ppb Os (Table 3).

Gold occurs as a native metal that contains Ag, Cu, Hg, and Te as impurities. Silver concentrates in sulfides and sulfosalts (up to 7.3 wt %). High Pt, Pd, and Os contents are typical of pyrite (sum of PGE = 760 ppb), wolframite (sum of PGE = 369 ppb), and molybdenite (sum of PGE = 82 ppb). Occurrence of Pt and Pd minerals is inferred.

Elevated contents of noble metals were established in concentrates obtained as products of ore processing.

(4) Contrasting zoning in the distribution of many chemical elements, carbon (graphite) and major economic and noble metals included, was revealed at the deposit. The lithophile rare elements, REE included, accumulate largely in the upper (frontal) geochemical zone, and the chalcophile elements, largely in the lower (back) zone. The siderophile elements are characterized by a poorly differentiated distribution.

The regular differences in concentrations of the same chemical elements in ore veins and greisen selvages are notable.

(5) Single- and two-phase fluid inclusions consisting of water and carbon dioxide are predominant. Three-phase inclusions that additionally contain solid phases (NaCl crystals and ore matter) are less abundant. The salinity of three-phase inclusions is 11.6–14.0 wt % NaCl equiv. The homogenization temperature of primary and secondary fluid inclusions is 290–340 and 140–160°C, respectively.

HCs (CH_4, C_2H_2, $C_2H_{4,6}$, C_3H_8, C_4H_{10}, C_5H_{12}, and C_6H_{14}) and free hydrogen are contained in the gases recovered from quartz of orebodies along with water and carbon dioxide. Orebodies are distinguished from one another by the composition of fluid inclusions.

The total fluid content in quartz from all orebodies regularly decreases with depth; thereby, the percentage of carbon dioxide relative to water and the degree of fluid reduction increase in the same direction, whereas the percentage of hydrogen relative to carbon decreases. In Vein 87, these variations in fluid composition are noted with an increase in the vein thickness.

The results of the fluid inclusion study testify to a sharp change in the parameters of the hydrothermal system in the zone of ore deposition. The ore formation

occurred under conditions of oxidation of an initially reduced metalliferous fluid.

(6) In accordance with the concept developed by Letnikov (2001, 2003; Letnikov and Dorogokupets, 2001), the data obtained indicate a deep character of the fluid–magmatic system responsible for the formation of the Kalguty deposit. In general, it should be noted that the effect of deep fluid increased during the evolution of this fluid–magmatic system and reached a maximum at the sulfide–sulfosalt–quartz substage of mineral formation.

ACKNOWLEDGMENTS

We thank V.A. Akimtsev, G.A. Babchenko, V.A. Ponomarchuk, A.A. Tomilenko, A.P. Shabanin, and O.S. Khmel'nikova for the analytical results and F.A. Letnikov for his constructive criticism and helpful advice. This study was supported by the program "Universities of Russia—Basic Research" (project no. UR 09.01.045) and the Russian Foundation for Basic Research (project no. 05-05-64356).

REFERENCES

1. I. Yu. Annikova, "Main Stages of Ore Formation and Their Relationships with Magmatism at the Kalguty Rare-Metal–Molybdenum–Tungsten Deposit in the Gorny Altai," in *Topical Problems of Geology and Mineralogy of Southern Siberia* (Inst. Geol. Mineral., Siberian Division, Russ. Acad. Sci., Novosibirsk, 2001), pp. 202–208 [in Russian].
2. I. Yu. Annikova, A. G. Vladimirov, S. A. Vystavnoi, et al., "The Kalguty Rare-Metal Granite Pluton (Gorny Altai): Geodynamic Setting, Subsurface Morphology, and Isotopic Age," in *Petrology of Igneous and Metamorphic Complexes* (Tomsk State Univ., Tomsk, 2002), Vol. 1, pp. 10–15 [in Russian].
3. V. B. Dergachev and E. I. Nikitina, "Water and Carbon Dioxide Content and the Kinetics of Their Extraction from Quartz at Tungsten Deposits of the Southeastern Gorny Altai," in *Mineralogy and Petrography of Rocks and Ores in the Main Mining Districts of Siberia* (Novosibirsk, 1983), pp. 18–27 [in Russian].
4. N. L. Dobretsov, "The Permian–Triassic Magmatism and Sedimentation in Eurasia As a Superplume Reflection," Dokl. Akad. Nauk **354** (2), 220–223 (1997) [Dokl. Earth Sci. **354** (4), 497–500 (1997)].
5. N. L. Dobretsov, "Mantle Plumes and Their Role in the Formation of Anorogenic Granitoids," Geol. Geofiz. **44** (12), 1243–1261 (2003).
6. M. S. Dresselhaus, M. A. Pimenta, and P. S. Eklund, *Raman Scattering in Materials Science* (Springer, New York, 2000).
7. G. Faure, *Principles of Isotope Geology*, 2nd ed. (Wiley, New York, 1986; Mir, Moscow, 1989) [in Russian].
8. A. F. Korobeinikov, *PGE Deposits of the World*, Vol. III: *Multicomponent Au–REE–PGE Deposits* (Nauchnyi Mir, Moscow, 2004) [in Russian].
9. E. V. Kuzhel'naya and V. B. Dergachev, "Vertical Zoning of Tungsten Deposits Located at Various Depths in the Gorny Altai," Geol. Geofiz. **31** (5), 59–67 (1990).
10. F. A. Letnikov, "Ultradeep Fluid Systems of the Earth and Problems of Ore Formation," Geol. Rudn. Mestorozhd. **43** (4), 291–307 (2001) [Geol. Ore Deposits **43** (4), 259–273 (2001)].
11. F. A. Letnikov, "Magma-Forming Fluid Systems of the Continental Lithosphere," Geol. Geofiz. **44** (12), 1262–1269 (2003).
12. F. A. Letnikov and P. I. Dorogokupets, "The Role of Superdeep Fluid Systems of the Earth's Core in Endogenic Geological Processes," Dokl. Akad. Nauk, **378** (4), 535–537 (2001) [Dokl. Earth Sci. **378** (4), 500–502 (2001)].
13. D.G. McCulloch, E.G. Gerstner, D.R. McKenzie, et al., "Ion Implantation in Tetrahedral Amorphous Carbon," Phys. Rev. B **52**, 850 (1995).
14. A. A. Potseluev and V. I. Kotegov, "Zoning and Proportions of Chemical Elements in Veins and Greisen Selvages, the Kalguty Deposit," Izv. Vyssh. Uchebn. Zaved., Geol. Razved., No. 4, 59–66 (2002).
15. A. A. Potseluev and V. I. Kotegov, "The Kalguty Fluid–Magmatic System, the Gorny Altai: Geochemical Evolution and Correlation," in *Modern Problems of Formation Analysis, Petrology, and Ore Potential of Igneous Rocks* (Siberian Division, RAS, 2003), pp. 268–269 [in Russian].
16. A. A. Potseluev, V. I. Kotegov, and V. A. Akimtsev, "Graphite from the Kalguty Rare-Metal Greisen Deposit, the Gorny Altai," Dokl. Akad. Nauk **399** (2), 241–244 (2004) [Dokl. Earth Sci. **399** (8), 1169–1171 (2004)].
17. A. A. Potseluev, V. I. Kotegov, and D. I. Babkin, "Rare Earth Elements in the Rocks from the Kalguty Deposit, the Gorny Altai," Izv. Tomsk Politekhn. Univ. **305** (6), 229–246 (2002).
18. A. A. Potseluev, A. Yu. Nikiforov, and V. I. Kotegov, "Outlooks of the Greisen-Type Ore at the Kalguty Deposit, the Gorny Altai," in *Regional Geology. Geology of Mineral Deposits* (Tomsk Polytechn. Univ., Tomsk, 2001), pp. 306–309 [in Russian].
19. V. I. Sotnikov, A. N. Berzina, M. Economou-Eliopoulos, and D. G. Eliopoulos, "Platinum and Palladium in Ores of Porphyry Copper–Molybdenum Deposits in Siberia and Mongolia," Dokl. Akad. Nauk **378** (5), 663–667 (2001) [Dokl. Earth Sci. **379** (5), 546–549 (2001)].
20. V. I. Sotnikov and E. I. Nikitina, *Molybdenum–Rare-Metal–Tungsten Greisen Deposits in the Gorny Altai* (Nauka, Novosibirsk, 1971) [in Russian].
21. S. R. Taylor and S. M. McLennan, *The Continental Crust: Its Composition and Evolution* (Blackwell, Oxford, 1985; Mir, Moscow, 1988).
22. A. G. Vladimirov, S. A. Vystavnoi, A. V. Titov, et al., "Petrology of the Early Mesozoic Rare-Metal Granitoids in the Southern Gorny Altai," Geol. Geofiz. **39** (7), 901–916 (1998).